ISSN:1738-6764, eISSN:2093-7504

Exact and Approximate Outage Analysis of Partial-CSI SWIPT Opportunistic AF Relay Networks over Rayleigh Fading

Kyunbyoung Ko [1] and Goo-Hyun Park [2,*]

[1] Dept. of Electronic Engineering, Korea National University of Transportation, Korea; kbko@ut.ac.kr
[2] GreenWave Radios (innophase), 163 Technology Drive, Suite 200 Irvine, CA 92618, USA; ghpark@innophaseinc.com
* Correspondence

https://doi.org/10.5392/IJoC.2025.21.4.020

Manuscript Received 10 November 2025; Received 24 December 2025; Accepted 24 December 2025

Abstract: *This work investigates the outage characteristics of a simultaneous wireless information and power transfer (SWIPT) opportunistic amplify-and-forward (OAF) relay network operating over Rayleigh fading channels. In the considered setup, each relay adopts a power-splitting (PS) protocol that divides the received radio-frequency signal for concurrent energy harvesting and data relaying. By formulating the partial channel state information (CSI)-based SWIPT OAF scheme as an equivalent generalized non-SWIPT relay model, tractable analytical expressions are derived to approximate the outage probabilities of both the indirect and combined transmission links, yielding reliable estimates of the true system behavior. Furthermore, an exact closed-form expression for the indirect link outage probability is obtained. Monte Carlo simulations confirm that the proposed analytical framework accurately captures the outage performance under a wide range of signal-to-noise ratio (SNR) conditions and relay selection scenarios. The developed analysis provides a convenient and insightful means for evaluating and optimizing SWIPT-assisted wireless sensor systems, thereby supporting their practical realization in energy-limited scenarios such as wireless sensor and Internet of Things (IoT) networks.*

Keywords: SWIPT; OAF Relay Network; PS; Partial-CSI; Outage Probability

1. Introduction

The increasing pursuit of sustainable and energy-conscious wireless communication has fueled intensive research on simultaneous wireless information and power transfer (SWIPT). In this paradigm, the radio-frequency (RF) waveform serves a dual purpose of conveying data and replenishing the energy of wireless devices [1-3]. SWIPT has become particularly attractive in cooperative relaying networks, where relays with limited energy resources harvest RF power and reuse it to forward information, thereby extending both network coverage and operational lifetime [4-10].

Among various receiver structures, the power-splitting (PS) approach has gained attention as a feasible means of dividing the received signal between energy harvesting (EH) and information processing (IP) [5], [9]. While PS improves flexibility in resource utilization, it also introduces significant analytical challenges when evaluating reliability metrics such as outage probability, which is highly sensitive to the nonlinear trade-off between EH and IP.

Recently, SWIPT systems incorporating simultaneous transmitting and reflecting reconfigurable intelligent surfaces (STAR-RIS) have emerged, where coordinated design of transmission, reflection, and power-splitting parameters yields notable improvements in both EH efficiency and throughput [11]. Concurrently, several studies have explored SWIPT-based amplify-and-forward (AF) relays, focusing on aspects such as optimal energy allocation [12], energy-aware relay selection [13], and the influence of hardware impairments or nonlinear EH circuits [14]. In addition, researchers have addressed outage behavior under various channel models. For instance, the authors in [15] examined SWIPT decode-and-forward (DF) relays

operating over correlated Nakagami-m fading, emphasizing how channel correlation deteriorates reliability. Similarly, the authors in [16] presented closed-form outage expressions for static fading scenarios, and the authors in [17] investigated partial-CSI relay selection in independent but non-identical distributed (INID) environments. Despite these efforts, most available analyses depend on restrictive assumptions or idealized setups, and only a few have rigorously characterized the outage probability of SWIPT-based opportunistic AF (OAF) relaying networks over INID fading channels [15-17].

Conversely, conventional AF relaying has been comprehensively investigated with respect to outage behavior, diversity enhancement, and relay selection mechanisms [18-22]. The opportunistic AF (OAF) strategy—where the relay offering the highest instantaneous end-to-end SNR forwards the source message—has been shown to improve link reliability and spectral efficiency [21-24]. However, when this principle is applied to SWIPT OAF relaying, the coupling between harvested energy and transmitted signal power introduces substantial analytical difficulty in deriving closed-form outage expressions.

While recent works such as [25, 26] have incorporated SWIPT into application-oriented frameworks (e.g., UAV-assisted or agricultural IoT networks), they primarily emphasize protocol design and empirical performance evaluation. A more fundamental outage analysis remains necessary to fully characterize the behavior of SWIPT OAF systems operating under partial channel state information (P-CSI).

To address this issue, prior studies [27-29] provide useful foundations. In [27], the authors analyzed error performance and derived a semi-analytical lower bound on capacity using a non-SWIPT equivalent model. Subsequently, in [28], this framework was generalized to OAF systems with P-CSI, where exact symbol error rate (SER) expressions were obtained. In [29], the channel capacity was analyzed. These results demonstrated the effectiveness of generalized non-SWIPT interpretations for performance evaluation.

Motivated by these observations, the present study investigates the outage probability characteristics of SWIPT-based OAF relaying networks under P-CSI conditions. By leveraging the generalized OAF framework, new analytical expressions are developed that explicitly capture the nonlinear interdependence between harvested energy and forwarded information—an aspect often simplified in existing models.

This paper offers the following main contributions:

- Derivation of new outage probability formulas using the generalized non-SWIPT interpretation framework.
- Comprehensive analytical and numerical evaluation of the effects of fading distribution, CSI availability, and relay selection threshold on reliability performance.
- Validation of the analytical results through Monte Carlo simulations, demonstrating their applicability to SWIPT-based wireless sensor and IoT networks.

The organization of the paper is as follows. Section 2 describes the system and channel models. Section 3 examines the outage probability for the source-to-relay (SR) link under partial CSI. Section 4 extends the analysis to the relay-to-destination (RD) link scenario. Section 5 presents simulation results that verify the proposed analytical derivations. Finally, Section 6 concludes the paper.

2. SWIPT OAF Relaying Networks under Partial-CSI

This section introduces the OAF relaying framework considered for SWIPT operation. We first describe the general system and signal models associated with the proposed scheme. Consider a cooperative network comprising a source, a destination, and R relays. The complex channel coefficients of the source–destination (SD), source–relay (SR), and relay–destination (RD) links are denoted by h_0, $\{h_r\}_{r=1}^{R}$, and $\{h_{R+r}\}_{r=1}^{R}$, respectively. All channels are modeled as statistically independent Rayleigh fading random variables.

Because each relay operates in half-duplex mode, data transmission occurs over two consecutive time slots. During the first slot, the source broadcasts an information-bearing signal x_s with $E[x_s] = 0$ and $E[|x_s|^2] = P_s$ to both the relays and the destination. The corresponding received signals at the rth relay and the destination are expressed as

$$y_r = h_r x_s + n_r \quad \text{and} \quad y_0 = h_0 x_s + n_0, \tag{1}$$

where n_r and n_0 represent independent additive white Gaussian noise (AWGN) terms with zero mean and variance σ^2. From (1), the instantaneous signal-to-noise ratio (SNR) of the direct link can be written as $\gamma_0 = P_s|h_0|^2/\sigma^2$, whose average value and channel power expectation are given by $\overline{\gamma_0} = P_s\Omega_0/\sigma^2$ and $\Omega_0 = E[|h_0|^2]$, respectively. The corresponding probability density function (PDF) is $f_{\gamma_0}(x) = \frac{1}{\overline{\gamma_0}}\exp\left(\frac{x}{\overline{\gamma_0}}\right)u(x)$, where $u(x)$ denotes the unit step function.

At each relay node, the received signal y_r is divided into two components to enable both EH and IP. Let ρ_r denote the PS ratio satisfying $0 < \rho_r < 1$ [2]. The portion of the signal dedicated to EH is $y_r^E = \sqrt{\rho_r} y_r = \sqrt{\rho_r}(h_r x_s + n_r)$. The harvested energy during the first slot is expressed as $E_r^h = E[|y_r^E|^2] = \eta \rho_r P_s |h_r|^2 T$, where $0 < \eta \leq 1$ denotes the energy conversion efficiency and T is the slot duration. Since AF relaying allocates equal durations to reception and transmission, the transmit power of the relay becomes $P_r = \eta \rho_r P_s |h_r|^2$.

The baseband signal reserved for information processing can be represented as

$$y_r^I = \sqrt{1-\rho_r}\ h_r x_s + n_{R_r}, \tag{2}$$

where $n_{R_r} = \sqrt{1-\rho_r}\ n_r + n_{c_r}$ and n_{c_r} denotes the conversion noise introduced during the radio frequency to baseband process. Both n_r and n_{c_r} are modeled as zero-mean independent Gaussian variables with variance σ^2, resulting in $\sigma_{R_r}^2 = (2-\rho_r)\sigma^2$.

During the second slot, each relay amplifies and retransmits the processed signal using its available transmit power P_r. Let the transmitted signal be $x_r = \kappa_r\ y_r^I$, where the amplification gain κ_r is defined as $\kappa_r = \sqrt{\frac{\eta \rho_r P_s |h_r|^2}{(1-\rho_r)P_s|h_r|^2 + \sigma_{R_r}^2}}$. Consequently, the destination receives from the rth relay

$$y_{R+r} = h_{R+r} x_r + n_{R+r}, \tag{3}$$

where n_{R+r} is the AWGN at the destination with variance σ^2. We can assume that all noise terms are mutually independent.

2.1 Received SNR of the Indirect Link

From (3), the instantaneous SNR of the indirect transmission path associated with the rth relay can be approximated for $\gamma_r \gg 1$ as [2], [27]

$$\gamma_{\ddot{u}_r} = \frac{\gamma_r \beta_r}{\beta_r + 1}, \tag{4}$$

where

$$\gamma_r = \frac{1-\rho_r}{2-\rho_r} \cdot \frac{P_s |h_r|^2}{\sigma^2} \quad \text{and} \quad \beta_r = \frac{2-\rho_r}{1-\rho_r} \cdot \eta \rho_r |h_{R+r}|^2 \tag{5}$$

and their respective averages are

$$\bar{\gamma}_r = \frac{1-\rho_r}{2-\rho_r} \cdot \frac{P_s\ \Omega_r}{\sigma^2} \quad \text{and} \quad \bar{\beta}_r = \frac{2-\rho_r}{1-\rho_r} \cdot \eta \rho_r \Omega_{R+r} \tag{6}$$

with $\Omega_r = E[|h_r|^2]$ and $\Omega_{R+r} = E[|h_{R+r}|^2]$.

2.2 Equivalent Modeling of a SWIPT OAF Relay as a General (Non-SWIPT) OAF Relay

Following the analytical approach in [27], the SWIPT OAF relay model can be approximated by an equivalent non-SWIPT OAF representation [28]. Under this approximation, the indirect link SNR $\gamma_{\ddot{u}_r}$ in (4) is rewritten as

$$\gamma_{\ddot{u}_r} = \frac{\gamma_r \beta_r}{\beta_r + 1} \approx \frac{\gamma_r \beta_r^{rd}}{\beta_r^{rd} + \gamma_r} \simeq \min\{\gamma_r, \beta_r^{rd}\} = \gamma_r^{OAF}, \tag{7}$$

where β_r^{rd} denotes a modified RD link SNR with PDF $f_{\beta_r^{rd}}(y) = \frac{1}{\bar{\beta}_r^{rd}} \exp\left(\frac{y}{\bar{\beta}_r^{rd}}\right) u(y)$. The mean value $\bar{\beta}_r^{rd}$, which depends on both $\bar{\gamma}_r$ and $\bar{\beta}_r$, is given by [27, 28]

$$\bar{\beta}_r^{rd} = \frac{1}{4} \frac{4\bar{\gamma}_r + 1}{4\bar{\gamma}_r} \frac{4\bar{\gamma}_r \bar{\beta}_r \frac{4\bar{\gamma}_r + 1}{4\bar{\gamma}_r}}{\log\left(4\bar{\gamma}_r \bar{\beta}_r \frac{4\bar{\gamma}_r + 1}{4\bar{\gamma}_r} + 1\right)} - \frac{1}{4}. \tag{8}$$

Note that for $\gamma_r \gg 1$, the above expression simplifies to $1/\left(4\bar{\beta}_r^{rd} + 1\right) \approx \log\left(4\bar{\gamma}_r \bar{\beta}_r + 1\right) / \left(4\bar{\gamma}_r \bar{\beta}_r\right)$ [27].

2.3 Relay Selection Strategy for SWIPT OAF Relaying under Partial-CSI

In the previous work [28], a relay selection protocol optimized for SWIPT OAF relaying was introduced. In this scheme, the source selects the optimal relay using partial-CSI of the SR links. Each relay transmits an identification signal powered by harvested energy, allowing the source to evaluate instantaneous SR link quality

and determine the relay index with the strongest channel. Prior to the power-splitting optimization step, all relays adopt an initial ratio $\rho_r = \rho_0 = 0.5$ to ensure stable SNR estimation during selection.

After the best relay is identified, it adjusts the power-splitting ratio to minimize the asymptotic bit error rate (BER) [27], which can be formulated as

$$\rho_{r,opt} = arg \min_{0<\rho_r<1} \left(\frac{1}{4\bar{\gamma}_r+1}, \frac{1}{4\bar{\beta}_r^{rd}+1}\right). \tag{9}$$

The stability and effectiveness of the optimized PS factor have been validated through both numerical computation and Monte Carlo simulation [27]. Although initially developed for error-rate analysis [28], this selection method also serves as a reliable foundation for outage evaluation in SWIPT-based relaying networks.

2. Outage Probability Analysis for SWIPT OAF Relaying under SR-Link Partial-CSI

The reliability of OAF relaying substantially decreases when the optimal relay is not properly chosen. As a preliminary analysis, the probability that the ith relay acts as the Nth best relay is first derived. Then, the outage characteristics of SWIPT-based OAF schemes are examined. For the indirect transmission path, both an exact closed-form and an approximated outage expression (derived from the generalized non-SWIPT AF framework) are presented, while for the combined link, only an approximate form is analytically tractable.

3.1 Selection Probability of the Nth Best SWIPT Relay

Let $\gamma_r^0 = \gamma_r|_{\rho_r=\rho_0}$ represent the SR-link SNR of the rth relay evaluated at an initial power-splitting ratio ρ_0. The index corresponding to the Nth best relay can be expressed as [30, 31]

$$i = arg \left(N_{th} \ \max\{\gamma_r^0\}_{r=1}^{R}\right), \tag{10}$$

where $arg \left(N_{th} \ \max\{\cdot\}\right)$ indicates the Nth order statistic among the R candidate relays. The selected relay employs the optimized power-splitting ratio $\rho_{i,opt}$ derived in (9) [27], and subsequently, the pair $\{\gamma_i, \beta_i\}$ is utilized for information transmission [28].

3.1.1 Derivation of the Selection Probability for the ith Relay

The selection rule in (10) corresponds to the Nth order statistic among R mutually independent random variables, implying that each relay possesses a non-zero probability of being identified as the Nth best. The PDF of this Nth order statistic associated with γ_r^0 can be expressed as

$$p_{\gamma_i^0}(x) = \sum_{j=1}^{\binom{R-1}{N-1}} \sum_{k=0}^{R-N} (-1)^k \sum_{l=1}^{\binom{R-N}{k}} \exp\left(-xB_i^{j,k,l}\right), \tag{11}$$

where

$$B_i^{j,k,l} = \sum_{p=1}^{N-1} \frac{1}{\bar{\gamma}_{\lambda_{i,p}^{N-1,j}}^0} + \sum_{m=1}^{k} \frac{1}{\bar{\gamma}_{\Gamma_m^{k,l}}^0}. \tag{12}$$

The full derivations of (11) and (12) are given in Appendix C of (29).

3.1.2 Joint Distribution for the Nth Best SWIPT Relay

Based on (10) and (11), the joint PDF of the Nth selected random variable pair $\{\gamma_i^0, \beta_i\}$ is written as [30]

$$f_{\gamma_i^0,\beta_i}^{N_{th}}(x,y) = \sum_{i=1}^{R} p_{\gamma_i^0}(x) f_{\gamma_i^0,\beta_i}(x,y) = \underbrace{\sum \cdots \sum}_{i,j,k,l} = \frac{\bar{\gamma}_i'(-1)^k}{\bar{\gamma}_i^0} \frac{1}{\bar{\gamma}_i} \exp\left(-\frac{x}{\bar{\gamma}_i}\right) \frac{1}{\bar{\beta}_i} \exp\left(-\frac{y}{\bar{\beta}_i}\right) u(x)u(y), \tag{13}$$

where the compact summation notation is defined as

$$\sum_{i=1}^{R} \sum_{j=1}^{\binom{R-1}{N-1}} \sum_{k=0}^{R-N} \sum_{l=1}^{\binom{R-N}{k}} = \underbrace{\sum \cdots \sum}_{i,j,k,l} \quad \text{and} \tag{14}$$

$$\frac{1}{\bar{\gamma}_i'} = \frac{1}{\bar{\gamma}_i^0} + B_i^{j,k,l}. \tag{15}$$

The parameter $\bar{\gamma}_i'$ is thus directly influenced by $B_i^{j,k,l}$ in (12).

The instantaneous SNR of the indirect path through the Nth best relay is given as

$$\gamma_{id}^{N_{th}} = \frac{\gamma_{N_{th}}\beta_{N_{th}}}{\beta_{N_{th}}+1}. \tag{16}$$

The joint PDF of $\{\gamma_{N_{th}}, \beta_{N_{th}}\}$ then follows as

$$f_{\gamma,\beta}^{N_{th}}(x,y) = \underbrace{\sum\cdots\sum}_{i,j,k,l} \frac{\bar{\gamma}_i^{(-1)^k}}{\bar{\gamma}_i^0} \frac{1}{\bar{\gamma}_i''} \exp\left(-\frac{x}{\bar{\gamma}_i''}\right) \frac{1}{\bar{\beta}_i} \exp\left(-\frac{y}{\bar{\beta}_i}\right) u(x)u(y) \tag{17}$$

with $\bar{\gamma}_i'' = (\bar{\gamma}_i/\bar{\gamma}_i^0)\bar{\gamma}_i'$.

From (17), the cumulative distribution function (CDF) of $\gamma_{id}^{N_{th}}$ is derived as

$$F_{\gamma_{id}^{N_{th}}}(z) = \underbrace{\sum\cdots\sum}_{i,j,k,l} \frac{\bar{\gamma}_i^{(-1)^k}}{\bar{\gamma}_i^0} \left[1 - \frac{2}{\bar{\beta}_i}\exp\left(-\frac{z}{\bar{\gamma}_i''}\right)\sqrt{\frac{\bar{\beta}_i z}{\bar{\gamma}_i''}}\ K_1\left(2\sqrt{\frac{z}{\bar{\gamma}_i''\bar{\beta}_i}}\right)\right] \tag{18}$$

where $K_1(\cdot)$ is the first-order modified Bessel function of the second kind [2], [32].

3.2 Exact Outage Probability for Direct and Indirect Link

An outage occurs when the instantaneous mutual information I is below the target transmission rate T_R. For the direct SD link occupying a single orthogonal channel,

$$I = \log_2(1+\gamma_0), \tag{19}$$

and thus

$$P_{out}^{sd} = Pr\{I \le T_R\} = F_{\gamma_0}\left(2^{T_R} - 1\right), \tag{20}$$

where $F_{\gamma_0}(x) = 1 - \exp\left(-\frac{x}{\bar{\gamma}_0}\right)u(x)$.

For OAF relaying, since two orthogonal channels are used,

$$I = \frac{1}{2}\log_2\left(1+\gamma_{id}^{N_{th}}\right), \tag{21}$$

and the corresponding outage probability from (18) is

$$P_{out}^{id} = F_{\gamma_{id}^{N_{th}}}\left(2^{T_R} - 1\right). \tag{22}$$

3.3 Approximation of SWIPT OAF Relaying to a General OAF Model

Following the approach in [27], the SWIPT OAF relay is approximated by a general OAF configuration to achieve comparable asymptotic BER [28], i.e., $\{\gamma_r, \beta_r\} \to \{\gamma_r, \beta_r^{rd}\}$.

3.3.1 Approximated PDFs and CDFs

For the indirect link, the Nth selected SNR is approximately presented as

$$\gamma_{id}^{N_{th}} = \frac{\gamma_{N_{th}}\beta_{N_{th}}}{\beta_{N_{th}}+1} \simeq \min\{\gamma_{N_{th}}, \beta_{N_{th}}^{rd}\} = \gamma_{id}^{OAF}. \tag{23}$$

The corresponding joint PDF is

$$f_{\gamma,\beta^{rd}}^{N_{th}}(x,y) = \underbrace{\sum\cdots\sum}_{i,j,k,l} \frac{\bar{\gamma}_i^{(-1)^k}}{\bar{\gamma}_i} \frac{1}{\bar{\gamma}_i''} \exp\left(-\frac{x}{\bar{\gamma}_i''}\right) \frac{1}{\bar{\beta}_i^{rd}} \exp\left(-\frac{y}{\bar{\beta}_i^{rd}}\right) u(x)u(y), \tag{24}$$

where $\bar{\beta}_i^{rd}$ is obtained from (8) by substituting $\bar{\gamma}_r \to \bar{\gamma}_i''$ and $\bar{\beta}_r \to \bar{\beta}_i^{rd}$.

Using the min-approximation [33], the PDF of γ_{id}^{OAF} becomes

$$f_{\gamma_{id}^{OAF}}(x) = \underbrace{\sum\cdots\sum}_{i,j,k,l} \frac{\bar{\gamma}_i^{(-1)^k}}{\bar{\gamma}_i} \frac{1}{\bar{\gamma}_i^{m\,in}} \exp\left(-\frac{x}{\bar{\gamma}_i^{m\,in}}\right) u(x), \tag{25}$$

where $\bar{\gamma}_i^{m\,in} = 1/\left(1/\bar{\gamma}_i'' + 1/\bar{\beta}_i^{rd}\right)$ [33].

Similarly, the combined-link SNR is approximated as

$$\gamma_{db}^{OAF} = \gamma_0 + \gamma_{id}^{OAF}. \tag{26}$$

and its PDF is

$$f_{\gamma_{cb}^{OAF}}(x) = \sum_{i,j,k,l}\cdots\sum \frac{\bar{\gamma}_i^{(-1)^k}}{\bar{\gamma}_i}\left[\frac{1}{\bar{\gamma}_0-\bar{\gamma}_i^{m\,n}}\exp\left(-\frac{x}{\bar{\gamma}_0}\right)+\frac{1}{\bar{\gamma}_i^{m\,n}-\bar{\gamma}_0}\exp\left(-\frac{x}{\bar{\gamma}_i^{m\,n}}\right)\right]u(x). \quad (27)$$

The CDFs are then written as

$$F_{\gamma_{id}^{OAF}}(z) = \sum_{i,j,k,l}\cdots\sum \frac{\bar{\gamma}_i^{(-1)^k}}{\bar{\gamma}_i}\left(1-\exp\left(-\frac{z}{\bar{\gamma}_i^{m\,n}}\right)\right)u(z) \quad (28)$$

and

$$F_{\gamma_{cb}^{OAF}}(x) = \sum_{i,j,k,l}\cdots\sum \frac{\bar{\gamma}_i^{(-1)^k}}{\bar{\gamma}_i}\left[\frac{\bar{\gamma}_0}{\bar{\gamma}_0-\bar{\gamma}_i^{m\,n}}\left(1-\exp\left(-\frac{z}{\bar{\gamma}_0}\right)\right)+\frac{\bar{\gamma}_i^{m\,n}}{\bar{\gamma}_i^{m\,n}-\bar{\gamma}_0}\left(1-\exp\left(-\frac{z}{\bar{\gamma}_i^{m\,n}}\right)\right)\right]u(x). \quad (29)$$

3.3.2 Approximated Outage Probabilities

Using (28), the outage probability of the indirect link can be approximated by

$$P_{out}^{id} \approx F_{\gamma_{id}^{OAF}}\left(2^{T_R}-1\right) = P_{out,id}^{OAF}. \quad (30)$$

Similarly, the outage probability of the combined link is obtained from (29) as

$$P_{out}^{cb} \approx F_{\gamma_{cb}^{OAF}}\left(2^{T_R}-1\right) = P_{out,cb}^{OAF}. \quad (31)$$

4. Outage Probability Analysis for SWIPT OAF Relaying under RD-Link Partial-CSI

This section investigates the relay selection mechanism utilizing P-CSI derived from the RD links [28].

4.1 Selection Probability of the Nth Best SWIPT Relay

We consider the scenario where relay selection is performed based on P-CSI obtained from the RD links. Let the set $\{\beta_r^0\}_{r=1}^R$ with $\beta_r^0 = \beta_r|_{\rho_r=\rho_0}$ represent the relay metrics; the selected relay index is given by

$$i = arg\ \left(N_{th}\ \ \max\{\beta_r^0\}_{r=1}^R\right), \quad (32)$$

where the destination chooses the Nth best relay prior to performing PS optimization [28].

Initially, all relays adopt with $\rho_r = \rho_0$, and after the selection, each relay adjusts its PS ratio independently, i.e., $\rho_i = \rho_{i,opt}$, to minimize the asymptotic BER. The resulting pair $\{\gamma_i, \beta_i\}$ is then used for the subsequent data transmission.

4.1.1 Derivation of the Selection Probability for the *i*th Relay

The selection procedure in (32) corresponds to the Nth order statistic among R independent random variables. Hence, any relay can potentially be selected as the Nth best.

Similar with (11), the PDF of β_i^0 is expressed as

$$p_{\beta_i^0}(x) = \sum_{j=1}^{\binom{R-1}{N-1}}\sum_{k=0}^{R-N}(-1)^k\sum_{l=1}^{\binom{R-N}{k}}\exp\left(-xB_i^{j,k,l}\right), \quad (33)$$

where

$$B_i^{j,k,l} = \sum_{p=1}^{N-1}\frac{1}{\bar{\beta}^0_{\lambda_{i,p}^{N-1,j}}}+\sum_{m=1}^{k}\frac{1}{\bar{\beta}^0_{\Gamma_m^{k,l}}}. \quad (34)$$

4.1.2 Joint Distribution for the *N*th Best SWIPT Relay

Based on (32) and (33), the joint distribution of the Nth best relay's parameters $\{\gamma_i, \beta_i^0\}$ can be expressed as

$$f_{\gamma,\beta^0}^{N_{th}}(x,y) = \sum_{i=1}^R p_{\beta_i^0}(x)\, f_{\gamma_i}(x) f_{\beta_i^0}(y) = \sum_{i,j,k,l}\cdots\sum \frac{\bar{\beta}_i^{(-1)^k}}{\bar{\beta}_i^0}\frac{1}{\bar{\gamma}_i}\exp\left(-\frac{x}{\bar{\gamma}_i}\right)\frac{1}{\bar{\beta}_i'}\exp\left(-\frac{y}{\bar{\beta}_i'}\right)u(x)u(y), \quad (35)$$

where $1/\bar{\beta}_i' = 1/\bar{\beta}_i^0 + B_i^{j,k,l}$. The indirect link SNR associated with the selected Nth best relay is $\gamma_{id}^{N_{th}} = \frac{\gamma_{N_{th}}\beta_{N_{th}}}{\beta_{N_{th}}+1}$. By applying the transformation $\beta_i^0 \to \beta_i$, the joint PDF of $\{\gamma_{N_{th}}, \beta_{N_{th}}\}$ is obtained as

$$f_{\gamma,\beta}^{N_{th}}(x,y)=\sum_{i,j,k,l}\cdots\sum\frac{\bar{\beta}_i(-1)^k}{\bar{\beta}_i^0}\frac{1}{\bar{\gamma}_i}\exp\left(-\frac{x}{\bar{\gamma}_i}\right)\frac{1}{\bar{\beta}_i''}\exp\left(-\frac{y}{\bar{\beta}_i''}\right)u(x)u(y), \tag{36}$$

where $\bar{\beta}_i''=\left(\bar{\beta}_i/\bar{\beta}_i^0\right)\bar{\beta}_i'$.

4.2 Exact Outage Probability for Indirect Link

For the chosen Nth best relay, the CDF of the indirect link SNR, $\gamma_{\dot{u}}^{N_{th}}$, can be computed as

$$F_{\gamma_{\dot{u}}^{N_{th}}}(z)=\sum_{i,j,k,l}\cdots\sum\frac{\bar{\beta}_i(-1)^k}{\bar{\beta}_i^0}\left[1-\frac{2}{\bar{\beta}_i''}\exp\left(-\frac{z}{\bar{\gamma}_i}\right)\sqrt{\frac{\bar{\beta}_i''z}{\bar{\gamma}_i}}\;K_1\left(2\sqrt{\frac{z}{\bar{\gamma}_i\;\bar{\beta}_i''}}\right)\;\right] \tag{37}$$

where $K_1(\cdot)$ is the first-order modified Bessel function of the second kind [2], [31].

The exact outage probability follows directly from (37) as

$$P_{out}^{\dot{u}}=F_{\gamma_{\dot{u}}^{N_{th}}}\left(2^{T_R}-1\right). \tag{38}$$

4.3 Approximation of SWIPT OAF Relaying to a General OAF Model

Following the approach in [27], the SWIPT OAF relay system can be represented approximately by a general OAF relay model.

4.3.1 Approximated PDFs and CDFs

Assuming the same conditions as in Section 3.3, the joint PDF becomes

$$f_{\gamma,\beta^{rd}}^{N_{th}}(x,y)=\sum_{i,j,k,l}\cdots\sum\frac{\bar{\beta}_i(-1)^k}{\bar{\beta}_i^0}\frac{1}{\bar{\gamma}_i}\exp\left(-\frac{x}{\bar{\gamma}_i}\right)\frac{1}{\bar{\beta}_i^{rd}}\exp\left(-\frac{y}{\bar{\beta}_i^{rd}}\right)u(x)u(y), \tag{39}$$

where $\bar{\beta}_i^{rd}$ is derived from (8) by substituting $\bar{\gamma}_r\;\rightarrow\bar{\gamma}_i$ and $\bar{\beta}_r\;\rightarrow\bar{\beta}_i'$.

Using the min-approximation [33], the PDF of the indirect kink SNR $\gamma_{\dot{u}}^{OAF}$ is expressed as

$$f_{\gamma_{\dot{u}}^{OAF}}(x)=\sum_{i,j,k,l}\cdots\sum\frac{\bar{\beta}_i(-1)^k}{\bar{\beta}_i^0}\frac{1}{\bar{\gamma}_i^{m\,\dot{n}}}\exp\left(-\frac{x}{\bar{\gamma}_i^{m\,\dot{n}}}\right)u(x), \tag{40}$$

where $\bar{\gamma}_i^{m\,\dot{n}}=1/\left(1/\bar{\gamma}_i+1/\bar{\beta}_i^{rd}\right)$ [32].

Using γ_0 and $\gamma_{\dot{u}}^{OAF}$, the PDF of the combined link SNR $\gamma_{\dot{c}\dot{b}}^{OAF}$ is

$$f_{\gamma_{\dot{c}\dot{b}}^{OAF}}(x)=\sum_{i,j,k,l}\cdots\sum\frac{\bar{\beta}_i(-1)^k}{\bar{\beta}_i^0}\left[\frac{1}{\bar{\gamma}_0-\bar{\gamma}_i^{m\,\dot{n}}}\exp\left(-\frac{x}{\bar{\gamma}_0}\right)+\frac{1}{\bar{\gamma}_i^{m\,\dot{n}}-\bar{\gamma}_0}\exp\left(-\frac{x}{\bar{\gamma}_i^{m\,\dot{n}}}\right)\right]u(x). \tag{41}$$

The corresponding CDFs are

$$F_{\gamma_{\dot{u}}^{OAF}}(z)=\sum_{i,j,k,l}\cdots\sum\frac{\bar{\beta}_i(-1)^k}{\bar{\beta}_i^0}\left(1-\exp\left(-\frac{z}{\bar{\gamma}_i^{m\,\dot{n}}}\right)\right)u(z) \tag{42}$$

and

$$F_{\gamma_{\dot{c}\dot{b}}^{OAF}}(z)=\sum_{i,j,k,l}\cdots\sum\frac{\bar{\beta}_i(-1)^k}{\bar{\beta}_i^0}\left[\frac{\bar{\gamma}_0}{\bar{\gamma}_0-\bar{\gamma}_i^{m\,\dot{n}}}\left(1-\exp\left(-\frac{z}{\bar{\gamma}_0}\right)\right)+\frac{\bar{\gamma}_i^{m\,\dot{n}}}{\bar{\gamma}_i^{m\,\dot{n}}-\bar{\gamma}_0}\left(1-\exp\left(-\frac{z}{\bar{\gamma}_i^{m\,\dot{n}}}\right)\right)\right]u(z). \tag{43}$$

4.3.2 Approximated Outage Probabilities

From (42), the indirect link outage probability can be approximated as

$$P_{out}^{\dot{u}}\;\approx F_{\gamma_{\dot{u}}^{OAF}}\left(2^{T_R}-1\right)=P_{out,\dot{u}}^{OAF}\,. \tag{44}$$

Similarly, from (43), the combined link outage probability is approximated using

$$P_{out}^{\dot{c}\dot{b}}\;\approx F_{\gamma_{\dot{c}\dot{b}}^{OAF}}\left(2^{T_R}-1\right)=P_{out,\dot{c}\dot{b}}^{OAF}\,. \tag{45}$$

5. Evaluation and Simulation Results

This section presents numerical evaluations of the proposed analytical expressions and validates them through Monte Carlo simulations. The simulations are carried out for the multi-relay SWIPT configuration shown in Section 2.

All simulations are implemented in MATLAB R2024a under the following setup. Binary phase-shift keying (BPSK, i.e., $M = 2$) is adopted, and all channels $\{h_r\}_{r=0}^{2R}$ are modeled as independent Rayleigh fading links. Each channel gain h_r has an average power $\Omega_r = E[|h_r|^2]$, corresponding to different channel environments. For statistical reliability, $\{h_r\}_{r=0}^{2R}$ the AWGN samples are independently generated 10^8 times. The noise at all receivers follows a complex Gaussian distribution with variance σ^2. The average SNR is defined as $\text{SNR} = \bar{\gamma}_0$ with $T_R = 1$ and $\eta = 0.8$.

In all plots, the blue and red lines denote the numerically derived results for the indirect link and the combined link, respectively. Simulation data labeled as 'Simulation' are obtained using the amplification gain $\kappa_r = \sqrt{\frac{\eta\rho_r P_S|h_r|^2}{(1-\rho_r)P_S|h_r|^2+\sigma_{R_r}^2}}$. For performance evaluation, two representative channel configurations are considered for the SWIPT OAF relay network with $R = 4$. In the first configuration, expressed as '$\text{Ch. Model} = [1, X, 1]$', the source–destination and relay–destination links are normalized to $\Omega_0 = 1$ and $\Omega_{R+r}|_{r=1}^{R} = 1$, respectively, while the source–relay link power levels vary as $\Omega_r \in \{0.5,1,2,4\}$. In the second configuration, denoted as '$\text{Ch. Model} = [1,1, X]$', both the source–destination and source–relay links are set to unity, and the relay–destination link power levels change as $\Omega_{R+r} \in \{0.5,1,2,4\}$. These two settings respectively emphasize the effect of channel variations on the SR and RD links while maintaining balanced power conditions for the other links.

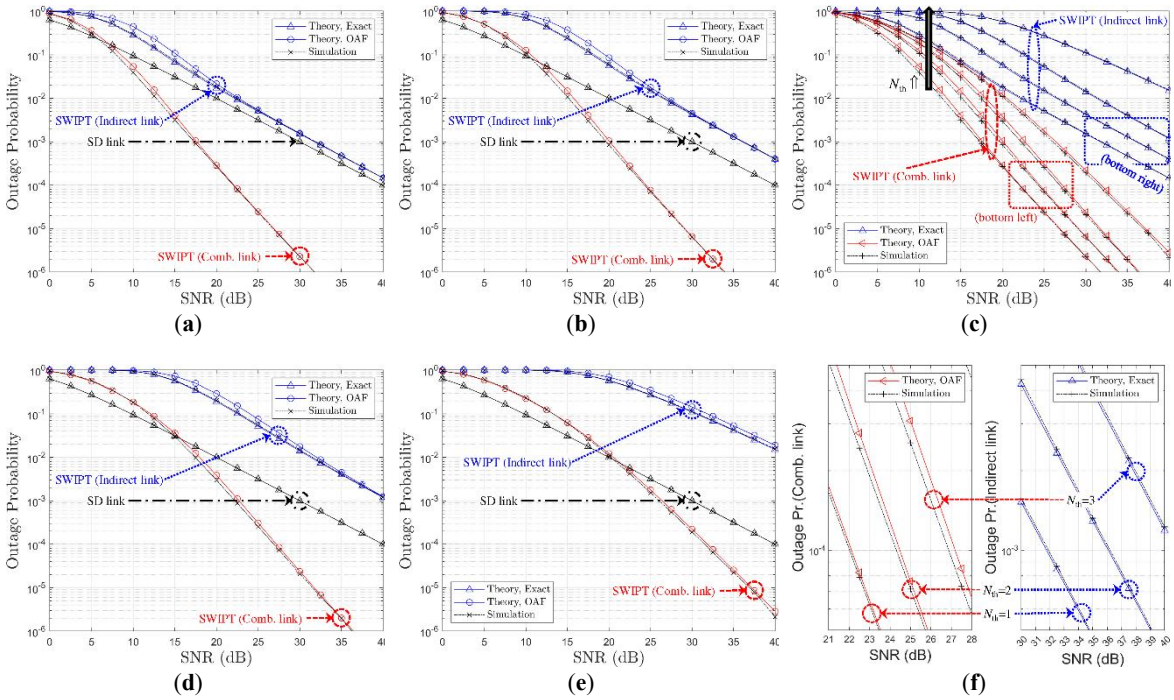

Figure 1. Outage probability performance of SWIPT OAF relaying systems versus SNR and Nth for SR-link CIS-based relay selection (BPSK modulation, $\rho_r = \rho_{opt}$, $N\text{th} = \{1,2,3,4\}$, $\text{Ch. Model} = [1, X, 1]$): (**a**) $N\text{th} = 1$; (**b**) $N\text{th} = 2$; (**c**) $N\text{th} = \{1,2,3,4\}$, both links; (**d**) $N\text{th} = 3$; (**e**) $N\text{th} = 4$; (**f**) $N\text{th} = \{1,2,3,4\}$, individual links.

5.1 SWIPT OAF Relaying with SR-Link-Based Partial-CSI

For the SR link under partial CSI, the exact outage probability $P_{out}^{\ddot{u}}$, labeled as 'Theory, Exact', is obtained from (22) with (18). Its OAF-based counterparts, $P_{out,\ddot{u}}^{OAF}$ and $P_{out,\ddot{c}b}^{OAF}$, labeled as 'Theory, OAF', are evaluated using (30) with (28), and (31) with (29), respectively. Figures 1-2 illustrate the outage probability versus the direct link SNR for various Nth, under '$\text{Ch. Model} = [1, X, 1]$' and '$\text{Ch. Model} = [1,1, X]$', respectively.

From Figures 1(a), 1(b), 1(d), and 1(e) (and Figures 2(a), 2(b), 2(d), and 2(e)), the indirect link performance is generally inferior to that of the direct link due to the relay's lack of a dedicated energy source. However,

when both links are combined, the SWIPT relaying scheme surpasses the direct link performance beyond a certain SNR level, which increases with Nth. The results marked 'Theory, OAF' match the simulated results well at medium and high SNR regions, while 'Theory, Exact' exhibits excellent accuracy across the entire range.

Figures 1(c) and 1(f) (and Figures 2(c) and 2(f)) highlight the effect of Nth on the SNR performance. As Nth increases, weaker relays with poorer link quality are more likely to be selected, thereby widening the gap between the direct and indirect links. This confirms that in OAF relaying, the selection diversity benefit mainly appears as an SNR enhancement rather than a diversity order improvement, unlike the case of full-CSI-based OAF systems.

Because relay selection here is based on SR-link CSI, the '$\mathrm{Ch.\,Model} = [1, X, 1]$' setup enables the system to select a relay with stronger SR conditions, leading to more efficient energy harvesting and improved RD performance. Hence, as seen in Figures 1(c) and 1(f), the outage curves under '$\mathrm{Ch.\,Model} = [1, X, 1]$' exhibit better performance than those under '$\mathrm{Ch.\,Model} = [1,1, X]$'.

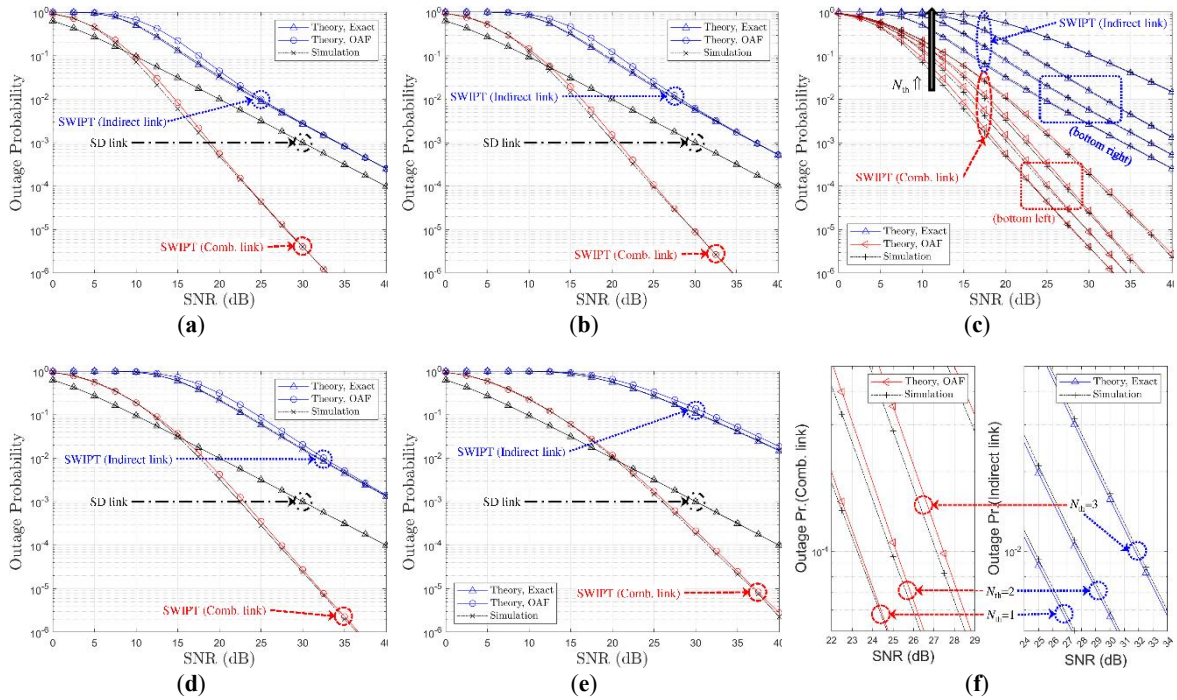

Figure 2. Outage probability performance of SWIPT OAF relaying systems versus SNR and *N*th for SR-link CIS-based relay selection (BPSK modulation, $\rho_r = \rho_{opt}$, $N\mathrm{th} = \{1,2,3,4\}$, $\mathrm{Ch.\,Model} = [1,1,X]$): (**a**) $N\mathrm{th} = 1$; (**b**) $N\mathrm{th} = 2$; (**c**) $N\mathrm{th} = \{1,2,3,4\}$, both links; (**d**) $N\mathrm{th} = 3$; (**e**) $N\mathrm{th} = 4$; (**f**) $N\mathrm{th} = \{1,2,3,4\}$, individual links.

5.2 SWIPT OAF Relaying with SR-Link-Based Partial-CSI

For the RD link under partial CSI, the exact outage probability $P_{out}^{\ddot{u}}$, labeled as 'Theory, Exact', is obtained from (38) with (37). Its OAF-based counterparts, $P_{out,\ddot{u}}^{OAF}$ and $P_{out,\ddot{b}}^{OAF}$, labeled as 'Theory, OAF', are evaluated using (44) with (42), and (42) with (43), respectively.

Figures 3 and 4 present the outage probability versus the direct link SNR for different Nth values, under '$\mathrm{Ch.\,Model} = [1, X, 1]$' and '$\mathrm{Ch.\,Model} = [1,1, X]$', respectively. The theoretical plots labeled as 'Theory, Exact' and 'Theory, OAF' show strong agreement with the simulated outcomes, especially in the moderate-to-high SNR regimes. Small deviations arise from the OAF approximation relying on asymptotic BER formulations.

As the RD-based selection uses only the RD-link SNRs, the '$\mathrm{Ch.\,Model} = [1,1, X]$' scenario favors the choice of stronger RD channels, thus providing an indirect-link SNR gain over '$\mathrm{Ch.\,Model} = [1, X, 1]$'. Accordingly, '$\mathrm{Ch.\,Model} = [1,1, X]$' represents a more favorable propagation setting for RD-link-based relay selection, consistent with the results observed in Section 5.1.

5.3 Comparative Analysis of SR- and RD-Link Relay Selection

By comparing Figures 1 and 3, and likewise Figures 2 and 4, the relative performance of SR- and RD-based selection strategies can be evaluated under different channel configurations. For both '$\mathrm{Ch.\,Model} = [1, X, 1]$' and '$\mathrm{Ch.\,Model} = [1,1, X]$' models, SR-based selection achieves comparable or superior outage results when $N\mathrm{th} = \{1,2,3\}$.

Figures 5 and 6 compare the outage probabilities between SR- and RD-based relay selections for '$\mathrm{Ch.\,Model} = [1, X, 1]$' and '$\mathrm{Ch.\,Model} = [1,1, X]$', respectively. In these plots, the blue and red curves denote the indirect and combined links, respectively. It is evident that the SR-based method consistently outperforms the RD-based approach for $N\mathrm{th} = \{1,2,3\}$.

This result implies that selecting a relay with a strong SR channel contributes more effectively to end-to-end reliability. Since SWIPT relays operate without an external power supply, choosing the optimal relay solely based on the RD link cannot fully utilize selection diversity, as energy harvesting fundamentally depends on the SR link quality. As a result, RD-based selection tends to yield higher outage probabilities, indicating that a stronger RD link does not necessarily ensure better performance for either the indirect link or the combined link when $N\mathrm{th} \leq 3$.

6. Conclusions

This study presented an outage probability analysis for SWIPT OAF relaying systems operating over Rayleigh fading channels, where relay selection was performed based on partial-CSI. Building upon the previously established analytical framework for generalized AF relay systems, approximate closed-form presentations were derived for the outage probabilities of both indirect and combined links, and the exact expression was obtained for the indirect link case. Monte Carlo simulation results confirmed that the proposed analytical approximations accurately capture the true outage probability under various SNR and channel conditions.

The analysis revealed that SR-link-based relay selection consistently provides superior performance compared to RD-link-based selection, primarily because of its direct influence on the relay's energy harvesting efficiency. The observed selection diversity benefits mainly translate into SNR improvements rather than gains in diversity order, which aligns with earlier findings in SWIPT error performance analyses. These outcomes offer valuable design insights for optimizing relay selection and power-splitting parameters in cooperative SWIPT relaying networks.

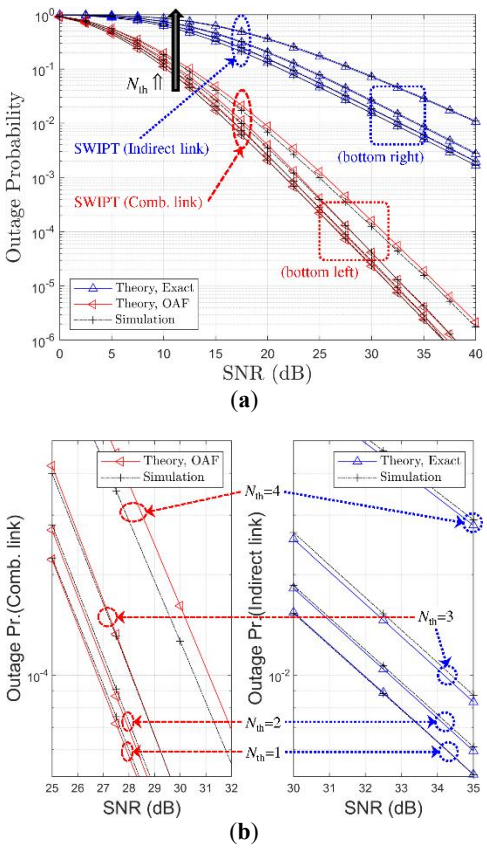

Figure 3. Outage probability performance of SWIPT OAF relaying systems versus SNR for RD-link CIS-based relay selection with power-splitting optimization (BPSK modulation, $\rho_r = \rho_{opt}$, $N\mathrm{th} = \{1,2,3,4\}$, $\mathrm{Ch.\,Model} = [1, X, 1]$): (**a**) both links; (**b**) individual links.

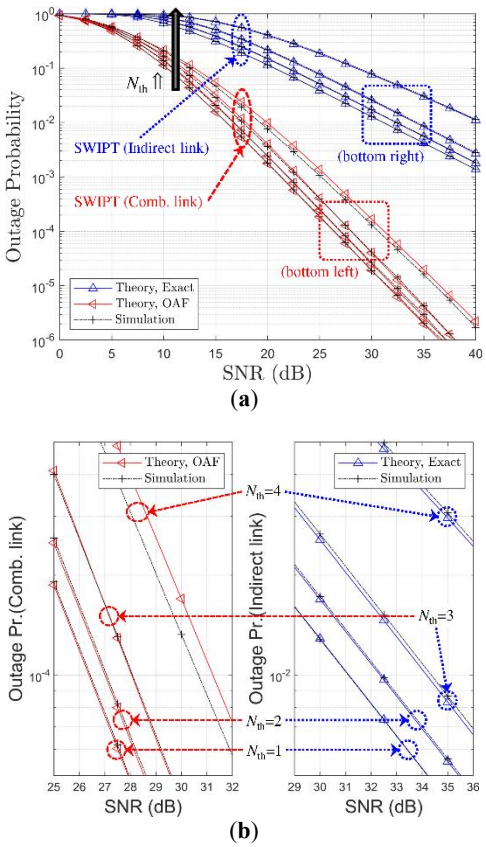

Figure 4. Outage probability performance of SWIPT OAF relaying systems versus SNR for RD-link CIS-based relay selection with power-splitting optimization (BPSK modulation, $\rho_r = \rho_{opt}$, $N\text{th} = \{1,2,3,4\}$, $\text{Ch. Model} = [1,1,X]$): (**a**) both links; (**b**) individual links.

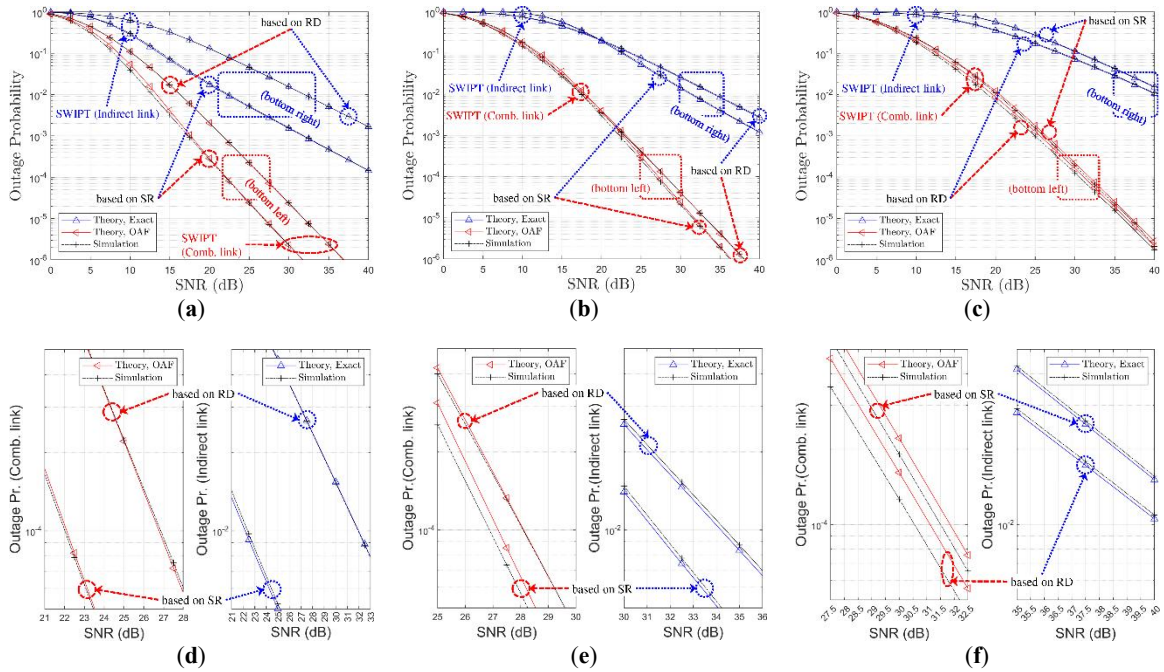

Figure 5. Outage probability performance of SWIPT OAF relaying systems versus SNR and *N*th for different relay selection strategies (BPSK modulation, $\rho_r \in \{0.5, \rho_{\text{opt}}\}$, $N\text{th} = \{1,3,4\}$, $\text{Ch. Model} = [1, X, 1]$): (**a**) $N\text{th} = 1$, both links; (**b**) $N\text{th} = 3$, both links; (**c**) $N\text{th} = 4$, both links; (**d**) $N\text{th} = 1$, individual links; (**e**) $N\text{th} = 3$, individual links; (**f**) $N\text{th} = 4$, individual links.

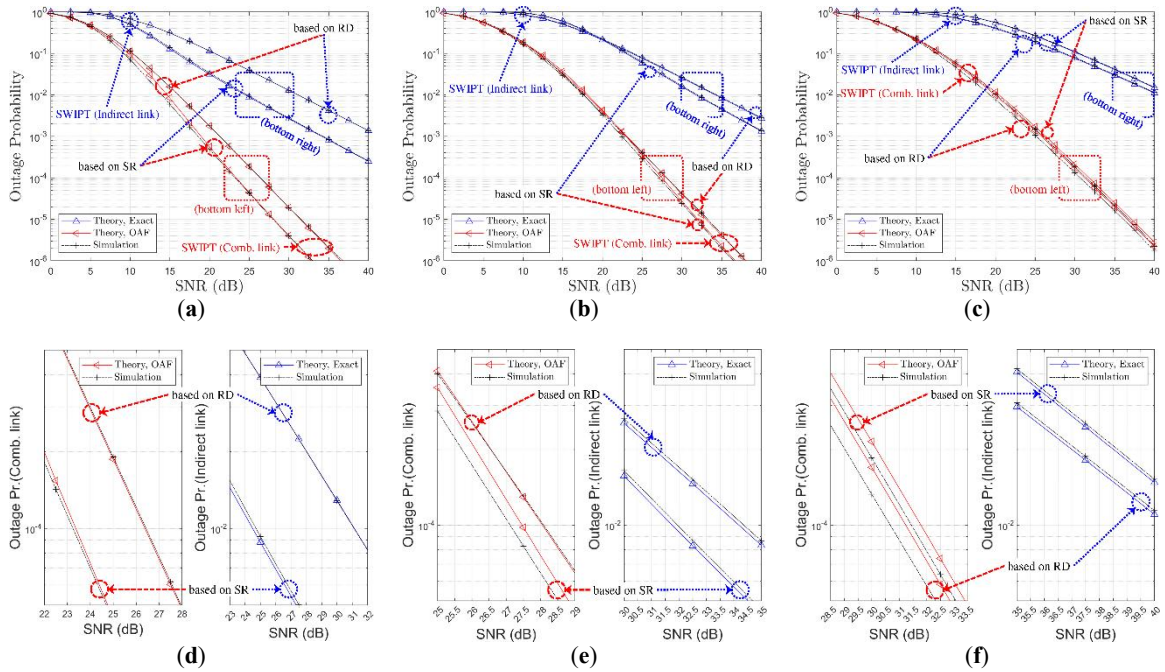

Figure 6. Outage probability performance of SWIPT OAF relaying systems versus SNR and Nth for different relay selection strategies (BPSK modulation, $\rho_r \in \{0.5, \rho_{\text{opt}}\}$, $N\text{th} = \{1,3,4\}$, $\text{Ch.Model} = [1,1,X]$): (**a**) $N\text{th} = 1$, both links; (**b**) $N\text{th} = 3$, both links; (**c**) $N\text{th} = 4$, both links; (**d**) $N\text{th} = 1$, individual links; (**e**) $N\text{th} = 3$, individual links; (**f**) $N\text{th} = 4$, individual links.

Acknowledgments: This research was supported by the Regional Innovation System & Education (RISE) program through the (Chungbuk Regional Innovation System & Education Center), funded by the Ministry of Education (MOE) and the (Chungcheongbuk-do), Republic of Korea (2025-RISE-11-004).

Conflicts of Interest: The authors declare no conflict of interest.

References

[1] 1. A. Nasir, X. Zhou, S. Durrani, and R. Kennedy, "Relaying Protocols for Wireless Energy Harvesting and Information Processing," IEEE Transactions on Wireless Communications, vol. 12, no. 7, pp. 3622–3636, 2013, doi: https://doi.org/10.1109/TWC.2013.062413.122042.

[2] H. Lee, C. Song, S. Choi, and I. Lee, "Outage Probability Analysis and Power Splitter Designs for SWIPT Relaying Systems with Direct Link," IEEE Communications Letters, vol. 21, no. 3, pp. 648–651, 2017, doi: https://doi.org/10.1109/LCOMM.2016.2627055.

[3] C. Song and Y. Jeon, "Weighted MMSE Precoder Designs for Sum-Utility Maximization in Multi-User SWIPT Network-MIMO With Per-BS Power Constraints," IEEE Transactions on Vehicular Technology, vol. 67, no. 3, pp. 2809–2813, 2018, doi: https://doi.org/10.1109/TVT.2017.2769139.

[4] H. Chen, X. Zhou, Y. Li, P. Wang, and B. Vucetic, "Harvest-Then-Cooperate: Wireless-Powered Cooperative Communications," IEEE Transactions on Signal Processing, vol. 63, no. 7, pp. 1700–1711, 2015, doi: https://doi.org/10.1109/TSP.2015.2396009.

[5] S. Mahama, D. K. P. Asiedu, and K. J. Lee, "Simultaneous wireless information and power transfer for cooperative relay networks with battery," IEEE Access, vol. 5, pp. 13171–13178, 2017, doi: https://doi.org/10.1109/ACCESS.2017.2724638.

[6] H. Lee, K. J. Lee, H. Kim, and I. Lee, "Wireless information and power exchange for energy-constrained device-to-device communications," IEEE Internet of Things Journal, vol. 5, no. 4, pp. 3175–3185, 2018, doi: https://doi.org/10.1109/JIOT.2018.2836325.

[7] S. He, K. Xie, W. Chen, D. Zhang, and J. Wen, "Energy-aware routing for SWIPT in multi-hop energy-constrained wireless network," IEEE Access, vol. 6, pp. 17996–18008, 2018, doi: https://doi.org/10.1109/ACCESS.2018.2820093.

[8] Z. Zhang, H. Pang, A. Georgiadis, and C. Cecati, "Wireless power transfer—An overview," IEEE Transactions on Industrial Electronics, vol. 66, no. 2, pp. 1044–1058, 2019, doi: https://doi.org/10.1109/TIE.2018.2835378.

[9] D. K. P. Asiedu, H. Lee, and K. J. Lee, "Simultaneous wireless information and power transfer for decode-and-forward Multi-hop Relay systems in energy-constrained IoT networks," IEEE Internet of Things Journal, vol. 6, no. 6, pp. 9413–9426, 2019, doi: https://doi.org/10.1109/JIOT.2019.2937090.

[10] Z. Liu, Y. Ye, G. Lu, and R. Q. Hu, "System Outage Performance of SWIPT Enabled Full-Duplex Two-Way Relaying With Residual Hardware Impairments and Self-Interference," IEEE Systems Journal, vol. 17, no. 1, pp. 337–348, 2023, doi: https://doi.org/10.1109/JSYST.2022.3145708.

[11] P. V. Quyet and H. H. Kha, "Max–Min Rate Optimization for STAR-RIS-Assisted SWIPT MIMO Cognitive Radio Systems," International Journal of Communication Systems, vol. 38, no. 10, Art. no. 70124, 2025, doi: https://doi.org/10.1002/dac.70124.

[12] K. Kim, D. K. P. Asiedu, P. Anokye, E. Kim, and K. J. Lee, "Transmit Power Optimization in Multihop Amplify-and-Forward Relay Systems with Simultaneous Wireless Information and Power Transfer," Electronics, vol. 13, no. 21, Art. no. 4232, 2024, doi: https://doi.org/10.3390/electronics13214232.

[13] S. Ghosh, T. Acharya, and S. P. Maity, "Outage Analysis in SWIPT Enabled Cooperative AF/DF Relay Assisted Two-Way Spectrum Sharing Communication," IEEE Transactions on Cognitive Communications and Networking, vol. 8, no. 3, pp. 1434–1443, 2022, doi: https://doi.org/10.1109/TCCN.2022.3171223.

[14] M. Babaei, L. Durak-Ata, and U. Aygolu, "Performance analysis of dual-hop AF relaying with non-linear/linear energy harvesting," Sensors, vol. 22, no. 16, Art. no. 5987, 2022, doi: https://doi.org/10.3390/s22165987.

[15] F. R. Ghadi and F. J. Lopez-Martinez, "Performance Analysis of SWIPT Relay Networks Over Arbitrary Dependent Fading Channels," IEEE Transactions on Communications, vol. 72, no. 6, pp. 3651–3663, 2022, doi: https://doi.org/10.1109/TCOMM.2024.3359034.

[16] D. Wang, R. Zhang, X. Cheng, and L. Yang "Capacity-Enhancing Full-Duplex Relay Networks based on Power-Splitting (PS-)SWIPT," IEEE Transactions on Vehicular Technology, vol. 66, no. 6, pp. 5445–5450, 2017, doi: https://doi.org/10.1109/TVT.2016.2616147.

[17] V. Panse, T. K. Jain, and A. Kothari, "Relay Selection in SWIPT-enabled Cooperative Networks," 2022 1st International Conference on the Paradigm Shifts in Communication, Embedded Systems, Machine Learning and Signal Processing (PCEMS), Nagpur, India, pp. 62–67, 2022, doi: https://doi.org/10.1109/PCEMS55161.2022.9807973.

[18] M. O. Hasna and M. S. Alouini, "End-to-End performance of transmission systems with relays over Rayleigh-fading channels," IEEE Transactions on Wireless Communications, vol. 2, no. 6, pp. 1126–1131, 2003, doi: https://doi.org/10.1109/TWC.2003.819030.

[19] P. A. Anghel and M. Kaveh, "Exact symbol error probability of a cooperative network in a Rayleigh-fading environment," IEEE Transactions on Wireless Communications, vol. 2, no. 5, pp. 1416–1421, 2004, doi: https://doi.org/10.1109/TWC.2004.833431.

[20] J. N. Laneman, D. N. C. Tse, and G. W. Wornell, "Cooperative diversity in wireless networks: Efficient protocols and outage behavior," IEEE Transactions on Information Theory, vol. 50, no. 12, pp. 3062–3080, 2004, doi: https://doi.org/10.1109/TIT.2004.838089.

[21] A. Bletsas, A. Khisti, D. P. Reed, and A. Lippman, "A simple cooperative diversity method based on network path selection," IEEE Journal on Selected Areas in Communications, vol. 24, no. 3, pp. 659–672, 2006, doi: https://doi.org/10.1109/JSAC.2005.862417.

[22] Y. Zhao, R. Adve, and T. J. Lim, "Symbol error rate of selection amplify-and-forward relay systems," IEEE Communications Letters, vol. 10, no. 11, pp. 757–759, 2006, doi: https://doi.org/10.1109/LCOMM.2006.060774.

[23] B. Maham and A. Hjorungnes, "Performance analysis of amplify-and-forward opportunistic relaying in Rician fading," IEEE Signal Processing Letters, vol. 16, no. 8, pp. 643–646, 2009, doi: https://doi.org/10.1109/LSP.2009.2021683.

[24] S. S. Ikki and M. H. Ahmed, "On the Performance of Cooperative-Diversity Networks with the Nth Best-Relay Selection Scheme," IEEE Transactions on Communications, vol. 58, no. 11, pp. 3062–3069, 2010, doi: https://doi.org/10.1109/TCOMM.2010.092810.090322.

[25] G. Lin, Y. Zhou, W. Jiang, X. He, X. Zhou, G. He, and P. Yang, "LF-SWIPT: Outage Analysis for SWIPT Relaying Networks Using Lossy Forwarding with QoS Guaranteed," IEEE Internet of Things Journal, vol. 9, no. 19, pp. 18737–18748, 2025, doi: https://doi.org/10.1109/JIOT.2022.3161980.

[26] Y. He, F. Huang, D. Wang, and R. Zhang, "Outage Probability Analysis of MISO-NOMA Downlink Communications in UAV-Assisted Agri-IoT With SWIPT and TAS Enhancement," IEEE Transactions on Network Science and Engineering, vol. 12, no. 3, pp. 2151–2164, 2025, doi: https://doi.org/10.1109/TNSE.2025.3545148.

[27] K. Ko and C. Song, "Error Performance Analysis and PS factor Optimization for SWIPT AF Relaying Systems over Rayleigh Fading Channels: Interpretation SWIPT AF relay as non-SWIPT AF relay," Electronics, vol. 14, no. 13, Art. no. 2597, 2025, doi: https://doi.org/10.3390/electronics14132597.

[28] K. Ko and S. Song, "Exact SER Analysis of Partial-CSI-Based SWIPT OAF Relaying over Rayleigh Fading Channels and Insights from a Generalized Non-SWIPT OAF Approximation," Sensors, vol. 25, no. 15, Art. no. 4872, 2025, doi: https://doi.org/10.3390/s25154872.

[29] K. Ko and S. Song, "Channel Capacity Analysis of Partial-CSI SWIPT Opportunistic Amplify-and-Forward (OAF) Relaying over Rayleigh Fading," Electronics, vol. 14, no. 19, Art. no. 3791, 2025, doi: https://doi.org/10.3390/electronics14193791.

[30] S. Nam, K. Ko, and D. Hong, "Exact Average SER Performance Analysis for the Nth Best Opportunistic Amplify-and-Forward Relay Systems," IEICE Transactions on Communications, vol. E95.B, no. 5, pp. 1852–1855, 2012, doi: https://doi.org/10.1587/transcom.E95.B.1852.

[31] K. Ko and C. Woo, "Outage Probability and Channel Capacity for Nth Best Relay Selection AF Relaying over INID Rayleigh Fading Channels," International Journal of Communication Systems, vol. 25, no. 11, pp. 1496–1504, 2012, doi: https://doi.org/10.1002/dac.1357.

[32] I. Gradshteyn and I. Ryzhik, Table of Integrals, Series and Products (7th ed., Academic Press, San Diego, CA, USA), 2007.

[33] S. Lim and K. Ko, "Approximation of Multi-hop Relay to Dual-hop Relay and Its Error Performance Analysis," IEEE Communications Letters, vol. 21, no. 2, pp. 342–345, 2017, doi: https://doi.org/10.1109/LCOMM.2016.2627054.